Long wavelength extension of CW-pumped supercontinuum through soliton-dispersive wave interactions

B. H. Chapman,[1,*] J. C. Travers,[1] S. V. Popov,[1] A. Mussot,[2] and A. Kudlinski[2]

[1]*Femtosecond Optics Group, Physics Department, Prince Consort Road, Imperial College, London SW7 2AZ, UK*

[2]*Laboratoire de Physique des Lasers, Atomes et Molécules (PhLAM), IRCICA, Université Lille 1, UMR CNRS 8523, 59655 Villeneuve d'Ascq Cedex, France*

http://www.femto.ph.ic.ac.uk

[*]*ben.chapman05@imperial.ac.uk*

Abstract: A supercontinuum spanning over 700 nm with an average spectral power of 1.7 mW/nm and flatness of 6 dB was produced in a solid core, double zero dispersion wavelength photonic crystal fiber pumped with a high power, continuous-wave ytterbium fiber laser. The spectrum displays a strong feature centered around 1980 nm. Through numerical simulations we demonstrate that this feature is initially generated through the shedding of Cherenkov radiation by solitons at the second zero dispersion wavelength, and then extended by a four-wave mixing process between this generated dispersive component and other solitons forming the continuum.

OCIS codes: (060.5530) Pulse propagation and temporal solitons; (190.4370) Nonlinear optics, fibers.

References and links

1. J. C. Travers, *Continuous wave supercontinuum generation* (Cambridge University Press, 2010), chap. 8.
2. A. V. Avdokhin, S. V. Popov, and J. R. Taylor, "Continuous-wave, high-power, Raman continuum generation in holey fibers," Opt. Lett. **28**, 1353–1355 (2003).
3. J. W. Nicholson, A. K. Abeeluck, C. Headley, M. F. Yan, and C. G. Jorgensen, "Pulsed and continuous-wave supercontinuum generation in highly nonlinear, dispersion-shifted fibers," Appl. Phys. B **77**, 211–218 (2003).
4. B. A. Cumberland, J. C. Travers, S. V. Popov, and J. R. Taylor, "29 W High power CW supercontinuum source," Opt. Express **16**, 5954–5962 (2008).
5. A. Kudlinski, G. Bouwmans, Y. Quiquempois, and A. Mussot, "Experimental demonstration of multiwatt continuous-wave supercontinuum tailoring in photonic crystal fibers," Appl. Phys. Lett. **92** (2008).
6. J. C. Travers, A. B. Rulkov, B. A. Cumberland, S. V. Popov, and J. R. Taylor, "Visible supercontinuum generation in photonic crystal fibers with a 400 W continuous wave fiber laser," Opt. Express **16**, 14435–14447 (2008).
7. B. A. Cumberland, J. C. Travers, S. V. Popov, and J. R. Taylor, "Towards visible CW pumped supercontinua," Opt. Lett. **33**, 2122–2124 (2008).
8. A. Kudlinski and A. Mussot, "Visible CW-pumped supercontinuum," Opt. Lett. **33**, 2407–2409 (2008).
9. A. Mussot and A. Kudlinski, "19.5 W CW-pumped supercontinuum source from 0.65 to 1.38 μm," Electron. Lett. **45**, 29–30 (2009).
10. J. C. Travers, "Blue solitary waves from infrared continuous wave pumping of optical fibers," Opt. Express **17**, 1502–1507 (2009).
11. A. Kudlinski, G. Bouwmans, O. Vanvincq, Y. Quiquempois, A. Le Rouge, L. Bigot, G. Mélin, and A. Mussot, "White light cw-pumped supercontinuum generation in highly GeO_2-doped-core photonic crystal fibers" Opt. Lett. **34**, 3631–3633 (2009).

#136831 - $15.00 USD Received 18 Oct 2010; accepted 4 Nov 2010; published 10 Nov 2010

12. P. Beaud, W. Hodel, B. Zysset, and H. Weber, "Ultrashort pulse propagation, pulse breakup, and fundamental soliton formation in a single-mode optical fiber," IEEE J. Quant. Electron. **23**, 1938–1946 (1987).
13. N. Nishizawa and T. Goto, "Characteristics of pulse trapping by ultrashort soliton pulse in optical fibers across zerodispersion wavelength," Opt. Express **10**, 1151–1160 (2002).
14. G. Genty, M. Lehtonen, and H. Ludvigsen, "Effect of cross-phase modulation on supercontinuum generated in microstructured fibers with sub-30 fs pulses," Opt. Express **12**, 4614–4624 (2004).
15. A. V. Gorbach and D. V. Skryabin, "Light trapping in gravity-like potentials and expansion of supercontinuum spectra in photonic-crystal fibres," Nat. Photonics **1**, 653–657 (2007).
16. J. M. Stone and J. C. Knight, "Visibly "white" light generation in uniform photonic crystal fiber using a microchip laser," Opt. Express **16**, 2670–2675 (2008).
17. A. Kudlinski, A. K. George, J. C. Knight, J. C. Travers, A. B. Rulkov, S. V. Popov, and J. R. Taylor, "Zero-dispersion wavelength decreasing photonic crystal fibers for ultraviolet-extended supercontinuum generation," Opt. Express **14**, 5715–5722 (2006).
18. N. Akhmediev and M. Karlsson, "Cherenkov radiation emitted by solitons in optical fibers," Phys. Rev. A **51**, 2602–2607 (1995).
19. D. V. Skryabin and A. V. Yulin, "Theory of generation of new frequencies by mixing of solitons and dispersive waves in optical fibers," Phys. Rev. E **72**, 016619 (2005).
20. A. Efimov, A. V. Yulin, D. V. Skryabin, J. C. Knight, N. Joly, F. G. Omenetto, A. J. Taylor, and P. Russell, "Interaction of an optical soliton with a dispersive wave," Phys. Rev. Lett. **95**, 213902 (2005).
21. A. V. Gorbach, D. V. Skryabin, J. M. Stone, and J. C. Knight, "Four-wave mixing of solitons with radiation and quasi-nondispersive wave packets at the short-wavelength edge of a supercontinuum," Opt. Express **14**, 9854–9863 (2006).
22. S. G. Johnson and J. D. Joannopoulos, "Block-iterative frequency-domain methods for maxwell's equations in a planewave basis," Opt. Express **8**, 173–190 (2001).
23. D. V. Skryabin, F. Luan, J. C. Knight, and P. St. J. Russell, "Soliton Self-Frequency Shift Cancellation in Photonic Crystal Fibers," Science **301**, 1705–1708 (2003).
24. F. Biancalana, D. V. Skryabin, and A. V. Yulin, "Theory of the soliton self-frequency shift compensation by the resonant radiation in photonic crystal fibers," Phys. Rev. E **70**, 016615 (2004).
25. J. C. Travers, F. M. H., and D. J. M., *Nonlinear fibre optics overview* (Cambridge University Press, 2010), chap. 3.
26. F. Vanholsbeeck, S. Martin-Lopez, M. González-Herráez, and S. Coen, "The role of pump incoherence in continuous-wave supercontinuum generation," Opt. Express **13**, 6615–6625 (2005).

1. Introduction

Continuous wave (CW) supercontinuum generation [1], is a proven route to high spectral power, spatially coherent sources across the infra-red [2–6] and visible spectral regions [6–10]. The interactions between solitons and dispersive waves are of particular interest in supercontinuum generation, as the shedding and trapping of dispersive 'Cherenkov' radiation across a zero dispersion wavelength (ZDW) can lead to the extension of the supercontinuum to shorter wavelengths [6–15], up to the visible [16] and even UV [17]. In double-ZDW fibers, dispersive waves can be generated across both ZDWs, allowing for the generation of un-trapped Cherenkov radiation at longer wavelengths [5, 7] and in this work we will show that the interaction between solitons with the generated Cherenkov radiation can lead to the generation of new spectral components in the long wavelength normal dispersion region, extending the supercontinuum.

It has long been understood that solitons under the influence of higher order dispersion can shed dispersive radiation through so-called 'Cherenkov' radiation [18]. This will occur where solitonic radiation is phase-matched to dispersive radiation within the soliton's spectrum, which is expressed by the phase-matching condition $\beta(\omega) = \beta_{\mathrm{sol}}(\omega)$, where the soliton propagation constant, β_{sol}, is the propagation constant of the soliton at the frequency of the dispersive wave, ω: $\beta_{\mathrm{sol}}(\omega) = \beta(\omega_{\mathrm{sol}}) + \beta_1(\omega_{\mathrm{sol}})[\omega - \omega_{\mathrm{sol}}] + \gamma P_0/2$. A number of recent papers have examined the interaction between solitons and co-propagating dispersive waves [19–21]. In the case of a soliton propagating with CW dispersive radiation at ω_{cw}, there will be two further matching conditions in addition to the Cherenkov condition, given by [21]:

$$\beta(\omega) = \beta(\omega_{\mathrm{cw}}) + \beta_{\mathrm{sol}}(\omega) - \beta_{\mathrm{sol}}(\omega_{\mathrm{cw}}) \tag{1}$$

$$\beta(\omega) = -\beta(\omega_{\mathrm{cw}}) + \beta_{\mathrm{sol}}(\omega) + \beta_{\mathrm{sol}}(\omega_{\mathrm{cw}}). \tag{2}$$

#136831 - $15.00 USD Received 18 Oct 2010; accepted 4 Nov 2010; published 10 Nov 2010

When expanded, Eq. (1) is seen to be independent of soliton power:

$$\beta(\omega) = \beta(\omega_{\rm cw}) + \beta_1(\omega_{\rm sol})[\omega - \omega_{\rm cw}]. \tag{3}$$

New frequency components will be created at resonances defined by roots of Eq.(3), which is understood as a four-wave mixing (FWM) process between the soliton and dispersive waves. This has been demonstrated both numerically [19], and experimentally [20], for the case of a single soliton interacting with a CW dispersive field. The contribution of this FWM process to the generation of short wavelengths in pulse-pumped supercontinua has been demonstrated experimentally in Ref. [21].

Here, we show experimentally, supported by numerical simulation, that the emission of Cherenkov radiation, and the subsequent interaction of solitons with this spectral component through the FWM process, can lead to spectral expansion of a CW-pumped supercontinuum to longer wavelengths. To the best of our knowledge, this is the first experimental observation of solitonic-dispersive wave interaction through FWM, leading to the generation of new frequencies, within the context of CW supercontinua.

2. Experimental setup

A 28 m length of solid core photonic crystal fiber was pumped using a high-power CW ytterbium fiber laser. Dispersion curves for the PCF (Fig. 1) were calculated from a scanning electron microscope (SEM) image of the fiber cross-section (Fig. 1 inset) using freely available software (MIT Photonic Bands [22]). The software suggests the fiber is slightly birefringent, but on both axes the dispersion curve has two ZDWs, at 0.82 μm and 1.84 μm.

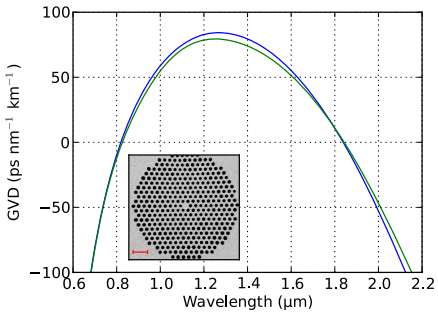

Fig. 1. Dispersion curves for both polarization axes of PCF, computed from SEM image of fiber cross section (inset, red bar indicates 5 μm scale)

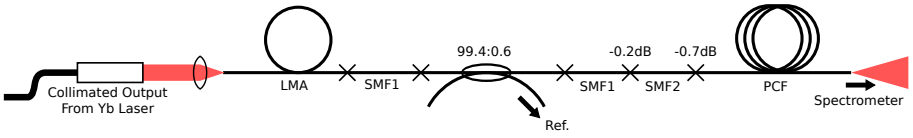

Fig. 2. Experimental set-up. Crosses indicate splices, fibers are as follows - LMA: large mode area fiber, SMF1: Corning HI-1060 single mode fiber, SMF2: Nufern small mode area single mode fiber

Figure 2 shows the set-up used to couple the pump into the PCF. To maximize coupling efficiency, the collimated output of the Yb fiber laser was coupled into large mode area (LMA fiber). The mode area was then stepped down through a cascade of fusion spliced single mode

#136831 - $15.00 USD Received 18 Oct 2010; accepted 4 Nov 2010; published 10 Nov 2010

fibers (SMF), so that it closely matched the small mode area of the PCF. The SMF cascade incorporated a 0.6% tap to act as a reference for the power coupled into the PCF. To avoid thermal damage to the reference tap and splices, the laser was on-off modulated at a repetition rate of 34 Hz and a switched-on time of 0.64 ms (giving a duty factor of 46). Pump powers stated hereafter are the effective (i.e. peak) pump power. The laser had a central wavelength of 1.07 μm and a 3 dB linewidth of 3 nm. The PCF was pumped with 133 W, and the spectrum of the output was recorded using a monochromator and an Indium Antinomide detector.

3. Results and discussion

Figure 3 shows the output from the PCF when pumped with 133 W. The spectral power axis is normalized to the total, time averaged, output power (i.e. a factor of 46, or 16 dB, lower than the instantaneous spectral power with the pump laser switched on). We see that a broad soliton-Raman continuum is been formed, exhibiting spectral flatness of 6 dB over 740 nm, from 1.08 μm to 1.82 μm, with an average spectral power of 1.73 mW/nm over this region. Taking into account the on-off modulation of the pump, this means that the average spectral power over this region was 80 mW/nm when the laser was on. Beyond the flat continuum there is a broad (80 nm FWHM) feature centered around 1.98 μm formed from the emission of dispersive radiation by solitons across the second ZDW. This feature is then further broadened to longer wavelengths through soliton-dispersive wave FWM, as discussed below. The linear scale plot of the spectrum shown as an inset in Fig. 3 illustrates more clearly that a significant amount of power has been transferred to this region beyond the second zero, and in fact this dispersive wave is the dominant spectral feature, containing 330 mW of power in an 80 nm bandwidth. Taking into account the modulation of the pump, this represents a conversion efficiency of 11% from the narrow 1.07 μm pump line to the broad 1.98 μm feature.

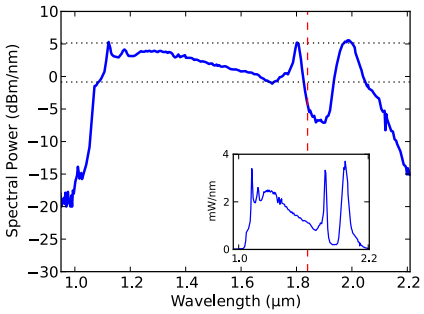

Fig. 3. Output spectrum from 28 m length of PCF normalized to time averaged output power on logarithmic and linear (inset) scale. Black dotted lines indicates 6 dB of spectral flatness over the 1.08 μm to 1.82 μm region, red dashed line indicates ZDW

To gain insight into the dynamics of the supercontinuum formation mechanism, a cut-back was performed along the fiber, with spectra taken at 2 m intervals from 28 back to 6 m, and 1 m intervals thereafter. The result of this cutback is shown as a density map of fiber length as a function of wavelength in Fig. 4a. The continuum is seen to quickly expand up to the second ZDW within the first meters. From $\sim$5 m, a feature is seen to form past 2 μm, filling in as the continuum extends to the second ZDW so that its peak is at 1.98 μm. The location of this feature matches well with the phasematching conditions for Cherenkov radiation by solitons just short of the ZDW. As soliton propagation requires anomalous dispersion, the solitons forming the continuum cannot self frequency shift past the ZDW and are halted just short, shedding dispersive radiation in the normal dispersion region [23, 24]. For propagation distances of $>$ 10 m

#136831 - $15.00 USD Received 18 Oct 2010; accepted 4 Nov 2010; published 10 Nov 2010

there is further expansion of the spectrum up to $\sim 2.2\ \mu$m.

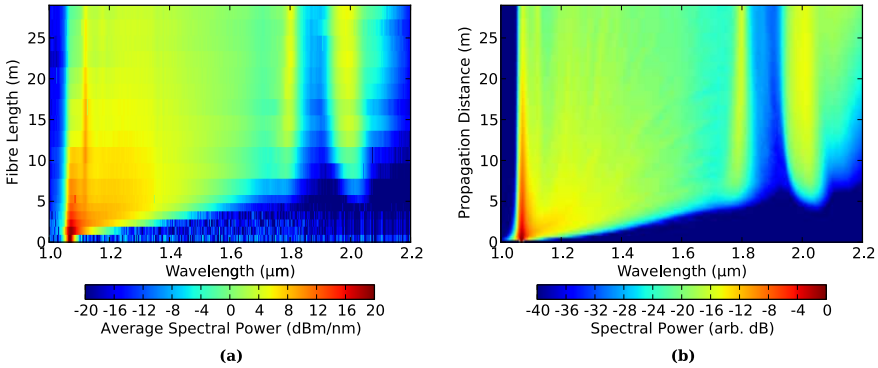

Fig. 4. Evolution of continuum with fiber length. **(a)** Results from experimental cut back along fiber length. **(b)** Simulation results, averaged from an ensemble of 100 shots.

The evolution of the spectrum along the fiber was simulated by solving the generalized nonlinear Schrödinger equation (GNLSE) along the full 28 m of fiber length using the split-step Fourier method [25]. It was assumed that the cross-polarization effects were negligible, and to account for the stochastic nature of the continuum generation process, 50 scalar simulations were performed independently on each axis, with a 66.5 W pump (i.e. and the pump radiation was assumed to be coupled equally into each axis). In each case the initial conditions were a sech^2 shaped spectral amplitude, closely corresponding to our pump laser, with a random spectral phase [26]. This ensemble of 100 shots was averaged and the results are shown in Fig. 4b.

Good agreement can be seen in Fig. 4 between the numerical results and the experiment. The most notable difference between the numerically calculated spectra and the experimentally measured spectra is the presence of a strong component at the first Raman Stokes order (around 1.12 μm) in the experimental results. A likely source for this disagreement is the fact that the numerical simulations only account for the forward propagating field. Empirically Raman scattering of the CW pump line may lead to backward propagating CW radiation at the first Raman order wavelength. The final input splice onto the PCF is also relatively lossy ($\sim$0.7 dB), meaning that potentially a significant amount of the backward propagating radiation may be reflected back down the fiber, seeding the formation of this Raman line. In addition, the absolute level and spectral extent of the soliton FWM generated extension of the long wavelength dispersive component is greater in the numerical results than the experimental. This is due to the omission of attenuation from the simulations while in actuality silica linear absorption and confinement losses rapidly increases with wavelength beyond 2 μm, strongly attenuating the long wavelength components. However, both the Cherenkov and soliton FWM components of the spectra agree in their relative power, spectral location and initial propagation distance for formation, illustrating the validity of the numerical results. With confidence that the simulations contain the essential physics of the experiment, we can use the numerical results to understand the expansion of the spectrum at the long wavelength edge.

The roots of Eq. (3) were found for soliton wavelengths up to 1.84 μm with ω_{cw} set to correspond with the peak of the Cherenkov radiation component at 1.98 μm. The resulting phase-matching curve is shown in Fig. 5. This curve suggests that FWM between solitons and the dispersive radiation generated through the Cherenkov process should lead to the generation of new frequency components beyond 2 μm. Spectrogram plots, generated from simulation data, show that it is indeed the soliton FWM process which results in the expansion of the spectrum. This is clearly exemplified in Fig. 6. First a soliton initially stops short of the ZDW,

#136831 - $15.00 USD Received 18 Oct 2010; accepted 4 Nov 2010; published 10 Nov 2010

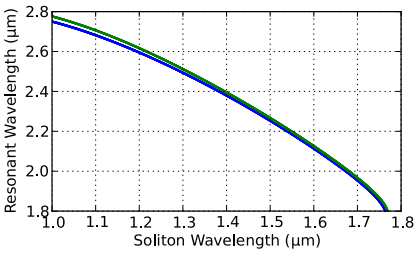

Fig. 5. Phase-matching curves derived from dispersion curves in Fig. 1 showing the resonant wavelengths for solitons mixing with dispersive radiation at 1.98 μm on the fast (blue) and slow (green) axis

resulting in the generation of a dispersive wave around 2 μm due to the Cherenkov process. The soliton and its dispersive wave are then delayed past a second soliton at a shorter wavelength, and new discrete spectral component is generated beyond the dispersive radiation, temporally collocated to the second soliton. The wavelength of the newly generated dispersive radiation matches the wavelength predicted by Eq. (3).

The agreement between the experimental and numerical results (Figs. 4a and 4b respectively), in terms of the spectral evolution with propagation distance, combined with the agreement with analytical predictions for the generation of long wavelength dispersive radiation through soliton FWM, strongly suggest that the extension of the Cherenkov radiation to longer wavelengths observed in the experimental results is indeed due to soliton FWM.

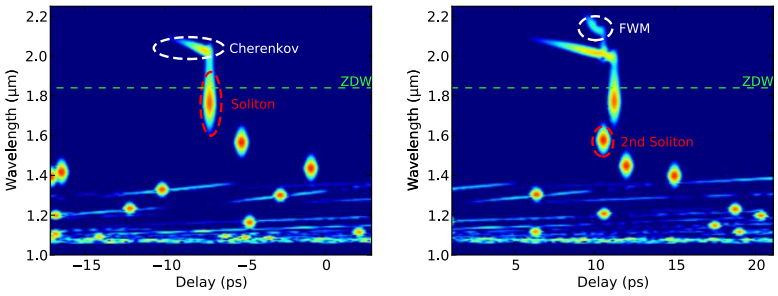

Fig. 6. Spectrograms produced from simulations. A soliton initially sheds dispersive radiation across the ZDW (left). The interaction of a second soliton with the dispersive radiation leads to the generation of a new spectral component (right).

4. Conclusion

Using a high power CW ytterbium fiber laser and a 28 m length of double ZDW PCF we generated a Raman-soliton supercontinuum with 6 dB spectral flatness over 740 nm, and an average spectral power of 1.7 mW/nm. In the normal dispersion region past the second ZDW, a broad (80 nm FWHM), high power (330 mW) feature with its peak at 1.98 μm was also observed. A cut-back was performed along the fiber which, along with numerical simulations, gave insight into the formation of the spectrum, in particular the region past the second ZDW.

The initial formation of the feature past the second ZDW is seen to be caused by Cherenkov radiation, while the further extension of this feature up to $\sim$ 2.15 μm is due to soliton FWM. This is, to the best of our knowledge, the first demonstration of soliton-dispersive wave FWM in the context of CW supercontinuum generation.

#136831 - $15.00 USD Received 18 Oct 2010; accepted 4 Nov 2010; published 10 Nov 2010